Proton MR Spectroscopic Imaging without Water Suppression[1]

Jan Willem C. van der Veen, PhD
Daniel R. Weinberger, MD
Gioacchino Tedeschi, MD
Joseph A. Frank, MD
Jeff H. Duyn, PhD

Index terms:
Brain, metabolism
Brain, MR, 10.12145
Magnetic resonance (MR) physics, 10.12145
Magnetic resonance (MR), pulse sequences, 10.12145
Magnetic resonance (MR), reconstruction algorithms, 10.12145
Magnetic resonance (MR), spectroscopy, 10.12145

Radiology 2000; 217:296–300

Abbreviations:
B_1 = radio-frequency magnetic induction field
B_0 = local constant magnetic induction field

[1] From the Clinical Brain Disorders Branch, National Institute for Mental Health (J.W.C.v.d.V., D.R.W.), and the Laboratory of Diagnostic Radiology Research (J.W.C.v.d.V., J.A.F., J.H.D.), National Institutes of Health, In Vivo NMR Research Center, Bldg 10, Room B1D125, 9000 Rockville Pike, Bethesda, MD 20892; and the Institute of Neurological Sciences, Second University of Naples, Italy (G.T.). From the 1999 RSNA scientific assembly. Received August 12, 1999; revision requested September 29; revision received December 28; accepted January 7, 2000. **Address correspondence to** J.W.C.v.d.V. (e-mail: *veen@nih.gov*).

Author contributions:
Guarantors of integrity of entire study, J.W.C.v.d.V., J.H.D.; study concepts, J.W.C.v.d.V.; study design, J.W.C.v.d.V., J.H.D.; definition of intellectual content, J.W.C.v.d.V., J.H.D.; literature research, J.W.C.v.d.V.; clinical studies, J.W.C.v.d.V., J.A.F., D.R.W.; data acquisition and analysis, J.W.C.v.d.V., J.H.D.; manuscript preparation, J.W.C.v.d.V., J.H.D.; manuscript editing, J.W.C.v.d.V., J.A.F., D.R.W., J.H.D.; manuscript review, all authors.

To improve reproducibility in proton magnetic resonance (MR) spectroscopic imaging in human brain, simultaneous acquisition of the internal water reference and metabolite signals was evaluated. Measurements in healthy volunteers showed that the increase in dynamic range from signal oversampling was sufficient to avoid digitization errors. In addition, use of singular value decomposition techniques and finite impulse response filters proved effective in separating water and metabolite signals and providing estimates of the metabolite concentrations.

The concentration of proton metabolites in human brain is generally in the millimolar range, which is several orders of magnitude lower than the 30–55 mol/L concentration of water. To facilitate the in vivo detection of these metabolites, proton magnetic resonance (MR) spectroscopic imaging typically includes some degree of suppression of the abundant water signals. There are two underlying reasons. First, water suppression reduces the dynamic range of the nuclear MR signal, thereby reducing dynamic range requirements on the receiver, specifically the preamplifier and the analog-to-digital converter. Second, water suppression potentially avoids the interference of water signals with metabolite signals, thereby facilitating data analysis.

Chemical-shift–selective saturation is among the most popular water-suppression techniques (1). Potential pitfalls of the chemical-shift–selective saturation pulse are interference with the metabolite signals owing to direct saturation effects and indirect saturation caused by magnetization-transfer effects on the metabolite resonances (1–4). To complicate matters, the magnitude of these effects is dependent on the homogeneity of the local constant magnetic induction field (B_0), which can become significant in MR spectroscopic imaging experiments owing to the relatively large variation in B_0 over the volume of interest.

Recent progress in the development and use of digital filters and analog-to-digital converters with high bandwidth (5,6) allows extension of the dynamic range of the receiver and acquisition of metabolite signals without water suppression (7). In this study, the combination of sophisticated data analysis methods, such as singular value decomposition (8–11), and high bandwidth of the analog-to-digital converter allowed simultaneous acquisition of both water and metabolite signals with a high degree of separation. This combination not only avoided the problems mentioned previously but also provided an additional advantage of use of the water signal as a reference signal to determine the metabolite concentrations in each voxel. This signal can be used for normalization and correction of instrumental imperfections such as eddy-current effects and inhomogeneities in B_0 and the radio-frequency magnetic induction field (B_1) (12–14). In addition, the reference signal could be used to calculate starting values for nonlinear curve fitting of the metabolite peaks.

The purpose of this study was to investigate in human brain the feasibility of simultaneous acquisition of internal water and metabolite signals and to determine whether the water and metabolite signals could be separated without distortion. A secondary goal was to determine the degree to which the metabolite signals were affected by a water-suppression pulse and to determine if an improvement in metabolite quantification could be obtained with proton MR spectroscopic imaging without water suppression.

Materials and Methods

Water-suppressed and non–water-suppressed proton MR spectroscopic imag-

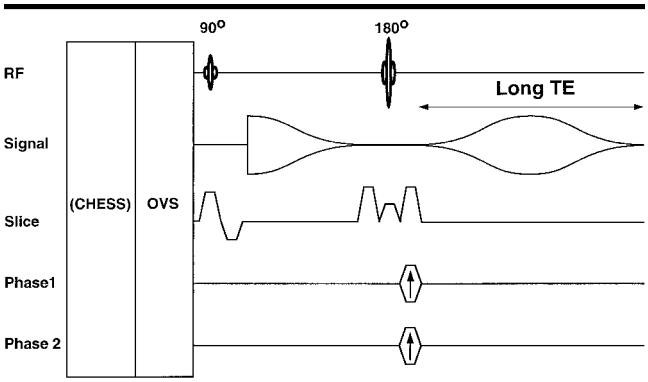

Figure 1. Pulse diagram for acquisition of multisection MR spectroscopic imaging data: *90°* is the 90° section-selective excitation pulse, and *180°* is the 180° refocusing pulse. The long echo time (*long TE*) spin-echo acquisition is preceded by an outer volume suppression (*OVS*) technique to suppress the lipids surrounding the brain and a water-suppression technique with chemical-shift–selective saturation (*CHESS*). The chemical-shift–selective saturation pulse was switched off for the non–water-suppressed images. *RF* = radio frequency.

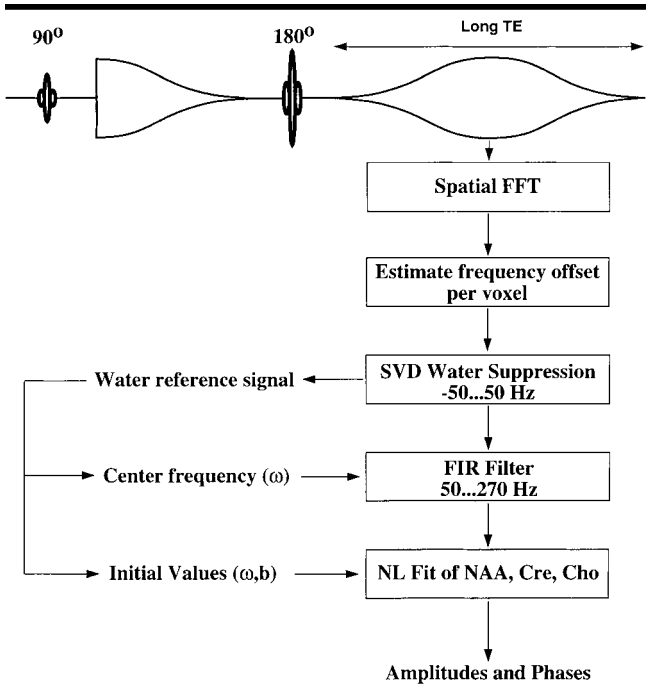

Figure 2. Overview of time-domain data analysis steps. After spatial Fourier transform (*FFT*), the time-domain signal analysis was started by estimating the local frequency offset in each voxel from the water signal. The water reference signal was then extracted from each signal by means of singular value decomposition (*SVD*) and used to provide secondary estimates for the local frequency offset (ω) and T2* (*b*). These estimates were then used to remove remaining water signal from the spectrum by means of a finite impulse response (*FIR*) filter and then to calculate initial values for a nonlinear (*NL*) fit of the *N*-acetylaspartate (*NAA*), choline (*Cho*), and creatine (*Cre*) resonances.

ing studies of the human brain were performed in five healthy volunteers (three men and two women; age range, 22–36 years; mean age, 27 years). Studies were performed with a 1.5-T MR imager (Signa; GE Medical Systems, Milwaukee, Wis) operating at the echo-speed platform with pulse-programming software. The system was equipped with shielded gradients (strength, 22 mT/m; slew rate, 120 T/m/sec) and a 16-bit digital receiver with a 125-kHz complex data sampling rate. The human subject protocol was approved by the intramural review board of the National Institutes of Health. Informed consent was obtained from each volunteer.

The MR spectroscopic imaging sequence consisted of three parts (Fig 1): (*a*) a chemical-shift–selective water-suppression pulse (1,15,16), (*b*) octagonal outer volume suppression (17) for suppression of the lipid signals from the skull and scalp, and (*c*) a spin-echo sequence for the MR spectroscopic imaging acquisition (18). For the non–water-suppressed experiments, the radio frequency and gradient crusher of water suppression with the chemical-shift–selective saturation were turned off. Four sections were measured in an interleaved fashion (order of 1, 3, 2, 4). The overall repetition time was 23,000 msec, and the echo time was 280 msec. Other imaging parameters included section thickness of 15 mm, section gap of 3.5 mm, 32 × 32 phase encoding over a 240 × 240-mm field of view, acquisition interval of 256 msec, and spectral bandwidth of 1 kHz. Sagittal scout images were acquired to aid positioning of the MR spectroscopic imaging sections. Preceding the MR spectroscopic imaging acquisition, automatic shimming and water-suppression calibration were performed over a single thick section that encompassed the four MR spectroscopic imaging sections.

With intensity differences between water and metabolite signals of up to 4,000:1 (19), a number of precautions have to be taken to avoid adding quantification noise to the acquired signal by using a dynamic range that is too small. An effective method to increase the dynamic range of the acquisition hardware is to oversample the signal by a large factor. The increase in bandwidth increases the noise amplitude while the spectroscopic signal amplitude remains unchanged. This results in a decrease in the dynamic range of the total signal. After acquisition, either the spectrometer hardware or data processing software can restore the original noise amplitude. A reduction in the number of sample points back to the original number by means of weighted averaging results in an increase in the dynamic range of the signal. In the current experiment, the hardware oversampled the signal by a factor of 125. Averaging a decimation filter (20) by a factor of 125 results in an increase in the coherent spectroscopic signal amplitude by 125, but the noise adds incoherently and is increased by a factor of only the square root of 125 (5,8). The signal-to-noise ratio is thus increased by a factor of

the square root of 125, or 11.18, and this increase adds approximately 4 bits to the dynamic range of the 16 bits of the analog-to-digital converter. The resultant total of 20-bit precision of a single acquisition point should be sufficient to cover the amplitude of the water signal and provide enough precision to quantize the noise without adding quantification noise. To preserve the additional bits from the decimation filter, the data have to be saved in a 32-bit format if the decimation filter is implemented with the imager hardware or with the "extended dynamic range" setting with the imager used in this study.

An additional concern with non–water-suppressed MR spectroscopic imaging is the signal-to-noise ratio of the preamplifier. Since the receiver gain needs to be reduced for non–water-suppressed MR spectroscopic imaging, the signal-to-noise ratio might suffer. According to manufacturer specifications and subsequent confirmation with measurements, however, patient noise appeared to dominate with the preamplifier settings used in these MR spectroscopic imaging experiments.

All data were analyzed with Sun SPARC workstations (Sun Microsystems, Mountain View, Calif) with IDL processing software (Research Systems, Boulder, Colo) according to the diagram in Figure 2. First, the data were Fourier transformed in the spatial dimension by means of cosine apodization (18) and double-precision spatial Fourier transform routines. Signals from individual voxels were subsequently analyzed in the time domain as follows: (*a*) a threshold at 30% of the maximum water amplitude was applied to the spectra, (*b*) the local B_0 value was determined by averaging the sample-to-sample phase increment of the non–water-suppressed signal, and (*c*) singular value decomposition of the signal was performed to separate water signals from metabolite signals (8) by selecting signal poles for singular value decomposition around the B_0 frequency offset in an interval of 100 Hz (1.57 ppm). From these methods, a water reference signal was reconstructed and subtracted from the original signal. In addition, the water reference signal was used to calculate a more precise estimate of the frequency offset. To further reduce the remaining water signal to avoid interference with the nonlinear fit of the metabolite signals, this offset was then used to center a 41-point finite impulse response filter (21) of 220 Hz around a frequency of 160 Hz (2.28 ppm), resulting in a transition band of 50–270 Hz (3.97–0.52 ppm, with the water resonance set at 4.75 ppm). Finally, nonlinear least squares fitting was performed with the standard IDL fitting routine known as "curvefit."

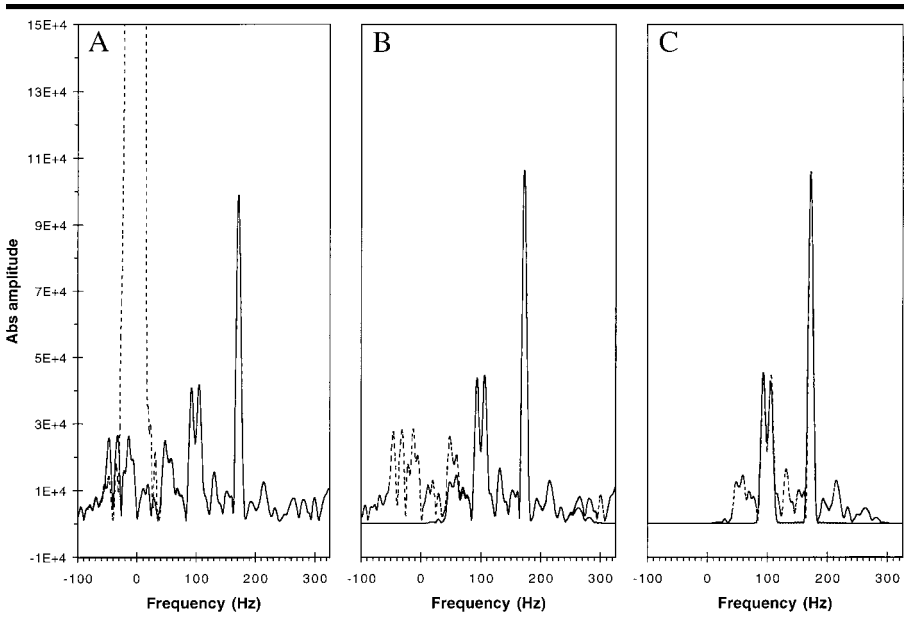

Figure 3. (*A–C*) Illustration of the data analysis steps for non–water-suppressed MR spectroscopic imaging. The data are displayed in spectral domain for clarity. *A*, *B*, Water signals are removed (dashed lines before, solid lines after) by means of singular value decomposition fitting and filtering by means of finite impulse response. *C*, The nonlinear fit (solid line) to the metabolite signals (dashed line) is illustrated. *Abs* = absolute.

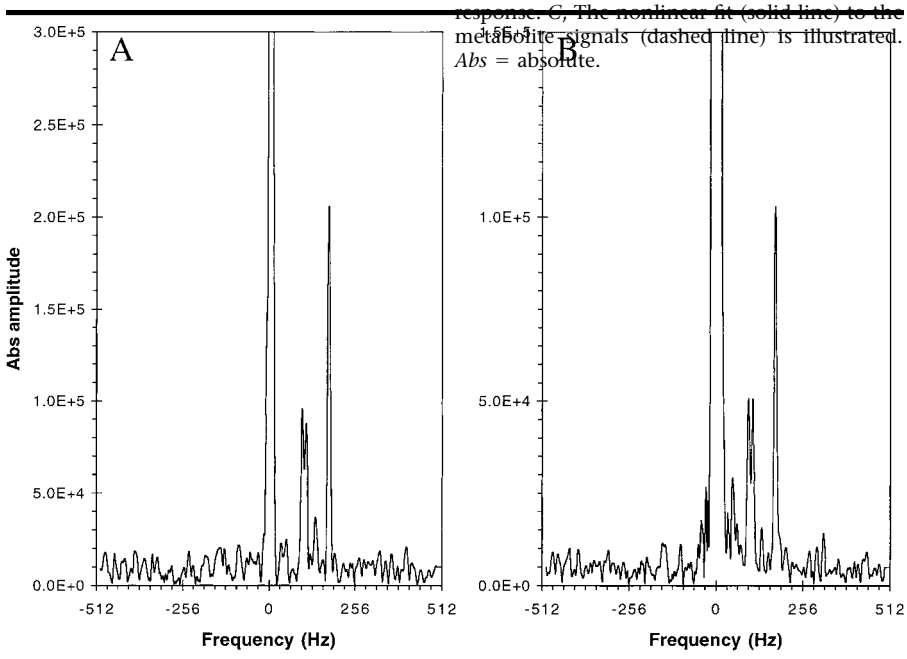

Figure 4. Spectra obtained both (*A*) with and (*B*) without water suppression. A Blackman apodization window was used to suppress the side lobes of the (residual) water signal. The non–water-suppressed signal was acquired with a gain reduction of a factor of two of the preamplifier value to accommodate the water signal. Note the similarity in the noise levels as compared with the metabolite amplitudes in both spectra. *Abs* = absolute.

The time-domain model function for each fitted metabolite signal consisted of three parts: (*a*) a complex exponential for the frequency offset, (*b*) an exponential damping term for T2, and (*c*) a Gaussian damping term symmetric around the echo top to model T2*. A single parameter was used for T2* of all the metabolite

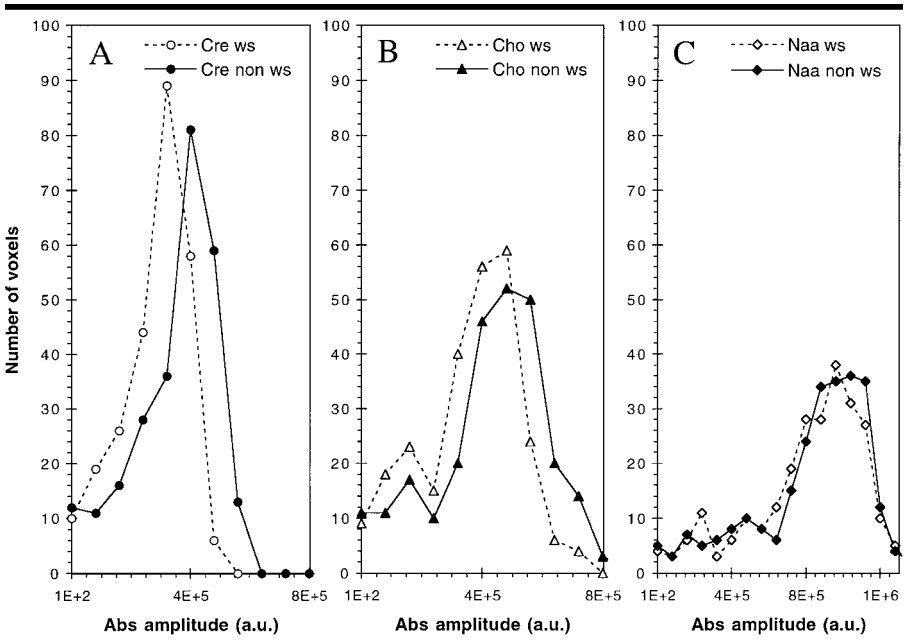

Figure 5. (*A–C*) Metabolite amplitudes in water-suppressed (*ws*) and non–water-suppressed (*non ws*) MR spectroscopic imaging. Histograms depict values found across a single brain section. Note the shift to lower amplitudes (horizontal axis) of the (*A*) creatine (*Cre*) and (*B*) choline (*Cho*) peaks in the water-suppressed data and the similar distributions in (*C*) *N*-acetylaspartate (*Naa*) values between the two experiments. *Abs* = absolute, *a.u.* = arbitrary units.

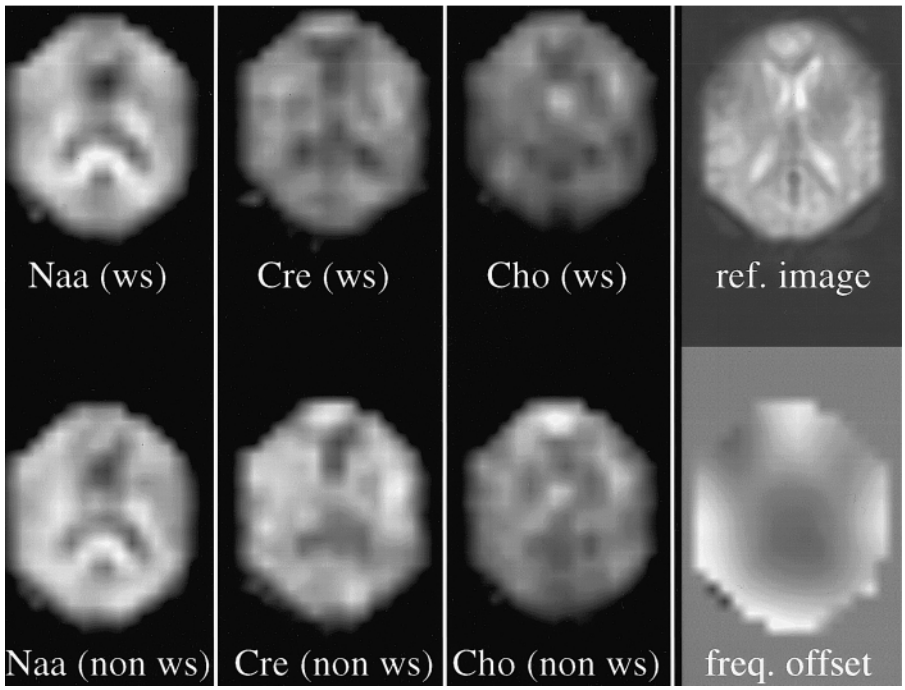

Figure 6. Metabolite images obtained with both water-suppressed (*ws*) and non–water-suppressed (*non ws*) MR spectroscopic imaging, together with a reference (*ref*) water image with higher spatial resolution and an image of frequency (*freq*) offset across the brain (B_0). Note the similar appearance of metabolite images obtained with or without water suppression. *Naa* = *N*-acetylaspartate, *Cho* = choline, *Cre* = creatine.

signals, but each frequency offset was fitted independently. Initial estimates of frequency offsets and T2* constants for the *N*-acetylaspartate, choline, and creatine signals were calculated from the water reference signal, and T2 constants were fixed at 270 msec for choline, 190 msec for creatine, and 300 msec for *N*-acetylaspartate (22,23). When the water-suppressed experimental data were analyzed, the water-subtraction procedure by means of singular value decomposition was omitted, and the initial estimates for the nonlinear fit, including the frequency offsets, were copied from the corresponding non–water-suppressed experiment.

Results

In our experiments, the maximum signal-to-noise ratio of the acquired signal ranged from 4,000 to 8,000. This signal-to-noise ratio depended on several experimental factors (eg, section thickness and location). Acquisition of a section through the ventricles with long T2 water resulted in a stronger signal than acquisition of a section through only brain tissue. Also, the size of the brain in the field of view was an important factor for maximum signal strength. The maximum signal-to-noise ratio of 8,000, or approximately 2^{13}, required 13–14 bits of the analog-to-digital converter, leaving only 2–3 bits for quantification of the noise. This was not sufficient to avoid adding quantification noise to the signal, and use of the additional 4 bits from the oversampling was required.

The MR spectroscopic imaging studies obtained without water suppression generally showed spectral quality and signal-to-noise ratio levels similar to those seen with water suppression. Inspection of the spectral data showed a consistently excellent fit of the water line and a virtual absence of water signal in the metabolite region after postprocessing. The effectiveness of analysis techniques in separating water signal from metabolite resonances is illustrated with a sample spectrum in Figure 3, which depicts the analysis steps in Figure 2. Although the data were analyzed in the time domain, they were displayed in the spectral domain for ease of interpretation. For this display, Blackman (Fig 3, *A*) and Hamming (Fig 3, *B*, *C*) apodizations were performed prior to spatial Fourier transform to suppress ringing effects. Figure 3, *A*, depicts the original signal and the signal after the water signal was removed by means of singular value decomposition. Figure 3, *B*, and 3, *C*, show the results of band pass filtering by means of finite impulse response and nonlinear metabolite fitting, respectively.

Figure 4 shows a comparison between typical spectra from a single voxel obtained with (Fig 4, A) or without (Fig 4, *B*) water suppression. The spectra were ob-

tained from the time-domain data before the spectral processing steps described previously and after Blackman apodization to suppress the side lobes of the nonsuppressed water signal. Both spectra were made in a single session with a single volunteer and taken from the same voxel location. Both acquisitions were made with the extended dynamic range setting but with a twofold difference in preamplifier gain. The water-suppressed signal was measured with maximum gain and the non–water-suppressed signal with a gain reduction of a factor of two to accommodate the additional signal from the water. The noise levels were measured within a 100-Hz range in the absolute value spectrum (−512 to −412 Hz). The two noise levels of 4,755 (non–water-suppressed) and 9,184 (water-suppressed) were equal within the SD of 15% and taking into account the amplification factor of two.

To investigate the effect of the water-suppression pulse on the amplitude of the metabolite signals, a histogram was created to compare absolute amplitude on the horizontal axis and the number of voxels with this amplitude on the vertical axis in experiments both with and without water suppression. The figure was calculated from all the voxels in a single section and from a single volunteer. The results (Fig 5) show good correspondence of *N*-acetylaspartate values between the water-suppressed and non–water-suppressed studies. However, both the choline and creatine resonances were markedly reduced in the experiment with water suppression. This could not be attributed to remaining water signals in the postprocessed non–water-suppressed spectra, because these were virtually absent. These results are suggestive of direct or indirect saturation of choline and creatine by means of the water-suppression pulse.

Figure 6 shows a qualitative comparison of metabolic images obtained both without and with water suppression, as well as a high-spatial-resolution reference image that outlines the position of the outer volume suppression sections and a B_0 map. For each metabolite, the intensity scale was kept constant for the two comparison images. Note the reduced intensity of the choline and creatine images in the water-suppressed experiment. Again, this could be related to the saturation effects of water suppression with the chemical-shift–selective saturation.

Discussion

Non–water-suppressed MR spectroscopic imaging appears feasible with state-of-the-art clinical imagers, provided that some precautions are taken. These precautions include efficient use of the full receiver bandwidth and sophisticated data analysis routines. The former can be achieved by means of digital filtering, either in the imager hardware or after acquisition in the data processing.

Omission of the water-suppression pulse eliminates the offset-dependent saturation of metabolite signals. This elimination is particularly important in studies with large volume coverage, such as MR spectroscopic imaging experiments. In these experiments, significant variations in the local field strength exist and metabolites closest to the water peak, such as myo-inositol and choline, are likely to be directly affected by the chemical-shift–selective saturation pulse. This saturation causes an additional variance in these metabolites between studies because of differences in frequency offset and water-suppression pulse calibrations. Also, there is a potential in water-suppressed experiments for indirect metabolite signal loss as a result of the magnetization-transfer effect, which is avoided when water suppression is omitted.

The water signal from the non–water-suppressed MR spectroscopic imaging experiment can be used for a number of purposes. First, it can provide initial estimates of resonance frequency and line width for spectral fitting routines. Second, it can be used as a navigator signal to correct for signal variations across image repetitions. Last, it can be used for normalization by allowing correction for imager imperfections such as inhomogeneities in B_1.

References

1. Haase A, Frahm J, Haenicke W, Matthei D. ^{1}H NMR chemical shift selective (CHESS) imaging. Phys Med Biol 1985; 30:341–344.
2. Bottomley PA, Foster TH, Leue WM. In vivo nuclear magnetic resonance chemical shift imaging by selective irradiation. Proc Natl Acad Sci U S A 1984; 81:6856–6860.
3. Luyten PR, Marien AJH, Heindel W, et al. Metabolite imaging of patients with intracranial tumors: H-1 MR spectroscopic imaging and PET. Radiology 1990; 176: 791–799.
4. Mescher M, Tannus A, Johnson MO, Garwood M. Solvent suppression using selective echo dephasing. J Magn Reson Series A 1996; 123:226–229.
5. Rosen ME. Selective detection in NMR by time-domain digital filtering. J Magn Reson Series A 1994; 107:119–125.
6. Redfield AG, Kunz SD. Analog filtering of large solvent signals for improved dynamic range in high-resolution NMR. J Magn Reson 1998; 130:111–118.
7. Hurd RE, Gurr D, Sailasuta N. Proton spectroscopy without water suppression: the oversampled J-resolved experiment. Magn Reson Med 1998; 40:343–347.
8. Pijnappel WWF, van den Boogaart A, de Beer R, van Ormondt D. SVD-based quantification of magnetic resonance signals. J Magn Reson 1992; 97:122–134.
9. de Beer R, Michiels F, van Ormondt D, van Tongeren BPO, Luyten PR, van Vroonhoven H. Reduced lipid contamination in in vivo ^{1}H MRSI using time-domain fitting and neural network classification. Magn Reson Imaging 1993; 11: 1019–1026.
10. Zhu G, Smith D, Hua Y. Post-acquisition solvent suppression by singular-value decomposition. J Magn Reson 1997; 124: 286–289.
11. Vanhamme L, Fierro RD, van Huffel S, de Beer R. Fast removal of residual water in proton spectra. J Magn Reson 1998; 132: 197–203.
12. Ordige RJ, Cresshull ID. The correction of transient B_0 field shifts following the application of pulsed gradients by phase correction in the time domain. J Magn Reson 1986; 69:151–155.
13. Morris GA. Compensation of instrumental imperfections by deconvolution using an internal reference signal. J Magn Reson 1988; 80:547–552.
14. Spielman D, Webb P, Macovski A. Water referencing for spectroscopic imaging. Magn Reson Med 1989; 12:38–49.
15. Doddrell DM, Galloway GJ, Brooks WM, et al. Water signal elimination in vivo, using "suppression by mistimed echo and repetitive gradient episodes." J Magn Reson 1986; 70:176–180.
16. van Zijl PCM, Moonen CTW. Solvent suppression strategies for in-vivo NMR. In: Diehl P, Fluck E, Günther H, Kosfeld R, Seelig J, eds. NMR, basic principles and progress 26. Berlin, Germany: Springer-Verlag, 1992; 67–108.
17. Duyn JH, Matson GB, Maudsley AA, Weiner MW. 3D phase encoding ^{1}H spectroscopic imaging of the human brain. Magn Reson Imaging 1992; 10:315–319.
18. Duyn JH, Gillen J, Sobering G, van Zijl PCM, Moonen CTW. Multisection proton MR spectroscopic imaging of the brain. Radiology 1993; 188:277–282.
19. Ernst T, Kreis R, Ross BD. Absolute quantitation of water and metabolites in the human brain. I. Compartments and water. J Magn Reson Series B 1993; 102:1–8.
20. Redfield AG, Kunz SD. Simple NMR input system using a digital signal processor. J Magn Reson Series A 1994; 108:234–237.
21. Oppenheim AV, Schafer RW. Digital signal processing. Englewood Cliffs, NJ: Prentice-Hall, 1975.
22. Frahm J, Bruhn H, Gyngell ML, Merboldt KD, Hanicke W, Sauter R. Localized proton NMR spectroscopy in different regions of the human brain in vivo: relaxation times and concentrations of cerebral metabolites. Magn Reson Med 1989; 11:47–63.
23. Christiansen P, Henriksen O, Stubgaard M, Gideon P, Larsson H. In vivo quantification of brain metabolites by ^{1}H-MRS using water as an internal standard. Magn Reson Imaging 1993; 11: 107–118.